A Magnetic and Mössbauer Study of the Layered Compound (NH$_4$)Fe(PO$_4$) · H$_2$O

J. E. GREEDAN, K. REUBENBAUER,* T. BIRCHALL, AND M. EHLERT

Department of Chemistry and Institute for Materials Research, McMaster University, Hamilton, Canada L8S 4M1

AND D. R. CORBIN AND M. A. SUBRAMANIAN

Central Research and Development Department, E. I. duPont de Nemours and Company, Experimental Station, Wilmington, Delaware 19898

(NH$_4$)Fe(PO$_4$) · H$_2$O was prepared using hydrothermal methods and studied using bulk magnetic and Mössbauer spectroscopic techniques. The compound appears to be isostructural with (NH$_4$)Co(PO$_4$) · H$_2$O and (NH$_4$)Cd(PO$_4$) · H$_2$O. Orthorhombic cell constants (Å) $a = 5.684(1)$, $b = 8.803(1)$, and $c = 4.818(5)$ were determined from powder data on highly oriented samples. The structure consists of FeO$_6$ layers stacked normal to the b-axis separated by NH$_4^+$ ions. Nominally polycrystalline samples were found to have a high degree of crystallographic orientation relative to the b-axis and the samples showed anisotropy in the magnetic and Mössbauer studies. Variable temperature susceptibility and magnetization studies from 300 to 4.2 K showed a Curie–Weiss region (nearly isotropic) to 80 K and a short-range ordered region to 26 K, below which long-range magnetic order occurs. The long-range order is characteristic of a uniaxial antiferromagnetic (b-axis preferred) with a remnant spontaneous moment due, presumably, to sublattice canting. The short-range regime gives evidence for antiferromagnetic interlayer and ferromagnetic intralayer exchange. Effective moments and Weiss constants derived from the paramagnetic data for the field parallel and perpendicular to the b-axis, respectively, were 5.33(5) μ_B, 5.41(5) μ_B and $-69(1)$ K, $-64(1)$ K. The temperature dependence of the Mössbauer hyperfine field ($H_{eff} = 22.3(1)$ at 6 K) showed the transition at 26 K to be of first order. The quadrupole splitting was strongly temperature dependent between 300 K (1.34(1) mm sec^{-1}) and 6 K (2.96(1) mm sec^{-1}) and η remained small (0.06(1) mm sec^{-1}) and constant over this range. The angle between V_{zz} and the hyperfine field direction was found to be 62(2)°. From an oriented sample the angle between V_{zz} and the b-axis was found to be 50(5)°. Thus, the hyperfine field makes an angle 12(5)° with the b-axis which is not inconsistent with the bulk magnetic data. © 1988 Academic Press, Inc.

Introduction

Crystal structures which have been reported for the divalent metal ammonium

* On leave from Institute of Nuclear Physics, PL-31-342 Cracow ul. Radzikowskiego 152, Poland.

monophosphate monohydrates, (NH$_4$)M(PO$_4$) · H$_2$O (M = Cd, Co, Fe, Mg, Mn, and Ni), indicate a layered arrangement of MO$_6$ octahedra separated by ammonium ions (*1, 3*) The oxygen atoms forming the octahedra about the M atoms are from the phosphate groups and the water of hydration.

Relatively few materials have been reported with this structure, possibly because hydrothermal synthetic methods are required. Such compounds containing transition metal ions would be good candidates for studies of low dimensional magnetism. The Fe^{2+} material is particularly interesting as Mössbauer spectroscopy can be used to provide microscopic site-specific information complementing bulk magnetic data. We have thus synthesized $(NH_4)Fe(PO_4) \cdot H_2O$ and carried out studies to elucidate its structure and magnetic properties.

Experimental

Synthesis

$(NH_4)Fe(PO_4) \cdot H_2O$ was prepared by a hydrothermal synthesis procedure in which a mixture of $Fe(CO)_5$, $(NH_4)_2HPO_4$, and H_2O was heated to 150°C for 48 h under autogenous pressure. The solvent and unreacted reactants were removed by filtering. The resulting solid was washed with acetone and water. Elemental analysis calcd for $(NH_4)Fe(PO_4) \cdot H_2O$ (wt%): Fe, 29.88; P, 16.57; N, 7.50; H, 3.24. Found: Fe, 29.12; P, 16.39; N, 7.29; H, 3.20. TGA showed a weight loss of 18.9% from 25 to 500°C on heating at 10°C/min in air. This loss corresponds to that expected for the loss of either 1 mole NH_3 or 1 mole H_2O.

X-Ray Powder Diffraction

Data on polycrystalline samples were obtained using a Nicolet I2 automated diffractometer. Lattice constants were refined from 15 unambiguously indexed reflections by least-squares analysis. Examination of the relative intensities indicated that the sample had a high degree of crystallographic orientation as will be discussed later.

Magnetic Measurements

Susceptibility and magnetization data were collected on pressed, highly oriented pellets with the applied field directed both parallel and perpendicular to the cylinder axis of the pellet. A PAR vibrating sample magnetometer was used.

Mössbauer

In an attempt to obtain the maximum amount of information from the Mössbauer experiment, and to be able to correlate this with X-ray and magnetic susceptibility measurements, two samples were prepared, one random and the other oriented. This latter being an effort to simulate the effect of a single crystal. The random sample was prepared by finely grinding the phosphate with sugar, which has an abrasive effect and separates the small crystallites, so that a random sample is obtained. This was then packed into a thin copper holder and sandwiched between scotch tape. The oriented sample was made by carefully packing down the flat platelets into the copper holder and then adding finely powdered sugar and pressing the two materials together, again between scotch tape, so that the phosphate crystallites could not move. Both samples contained 10 mg iron/cm².

Mössbauer spectra were measured using an Elscint transducer and waveform generator in conjunction with a CMTE manufactured MCD/PC microprocessor unit coupled to an IBM-AT microcomputer. A Kr-filled proportional counter was used to detect the γ-ray line and a Canberra or Aptec ADC/single channel analyzer was used to select the energy of interest and to measure the background under the γ-ray line. The low-temperature measurements were made in a cryostat manufactured by Technology Systems Inc. and the temperature was monitored by a silicon diode sensor and controlled by a Thor controller. The source, $^{57}Co/Rh$, was maintained at room temperature throughout. The spectrometer was calibrated using a standard foil of α-iron and all isomer shifts are refer-

enced against this material as having zero shift. Off-line folded spectra were fitted within the transmission integral approximation using the GMFP5ST program written by Reubenbauer and Birchall (4) which applies exact Hamiltonian diagonalization and spherical tensor elements describing the orientation of crystallites. The background under the γ-ray line was calculated for each geometry setting in order to estimate the effective recoilless fraction of the source and therefore provide realistic input parameters for the transmission integral approximation. Computations were carried out on a VAX-8600 computer.

Results and Discussion

Crystal Structure and Crystallographic Orientation

No crystals of a size suitable for structure determination were obtained. A scanning electron micrograph of typical crystal is shown in Fig. 1. The crystals are very thin plates with a largest dimension on the order of a few microns. Evidently, materials of this composition $(NH_4)M(PO_4) \cdot H_2O$ with M = Mg, Mn, Fe, Co, Ni, and Cd, can exist in two polymorphs (3). The relationship between the two is rather subtle and concerns whether the octahedra in adjacent layers have identical orientation, polymorph A, or inverted orientation, polymorph B (3). The space groups for A and B are $Pmn2_1$ and $Pnma$, respectively, and the unit cell orientations are such that $a_A \approx b_B$, $b_A \approx \frac{1}{2}a_B$, and $c_A \approx c_B$. The earliest structural report on these materials indicated the $Pmn2_1$ polymorph (1). All lines in the X-ray powder pattern of the $(NH_4)Fe(PO_4) \cdot H_2O$ sample prepared in this study could be indexed on a $Pmn2_1$ cell with $a = 5.684(1)$, $b = 8.803(1)$, and $c = 4.818(5)$ Å in reasonable agreement with Ref. (2), $a = 5.660(3)$, $b = 8.819(5)$, and $c = 4.827(3)$ Å. There was no evidence from the X-ray powder data for the existence of the $Pnma$ polymorph.

From the plate-like habit of the crystals, it was not surprising to find that nominally polycrystalline samples mounted on flat glass slides show considerable texture or
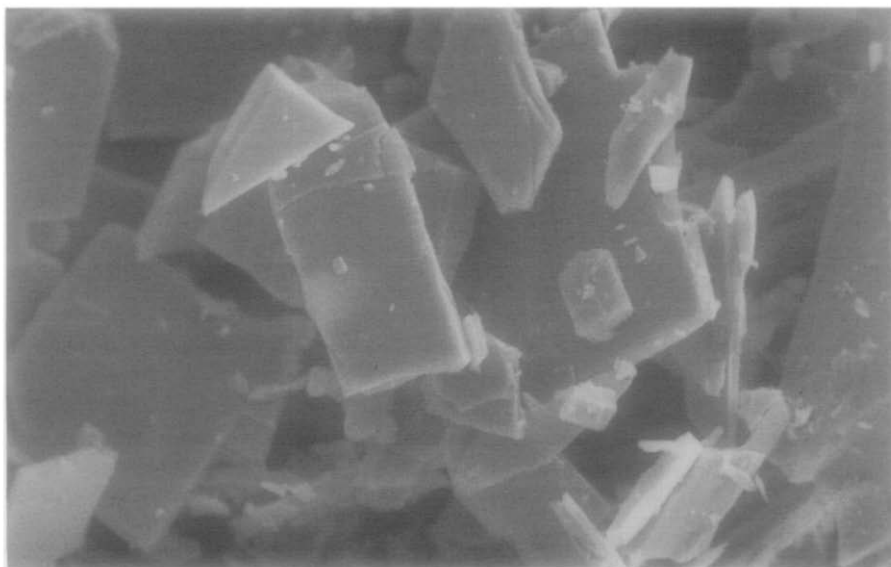

FIG. 1. Scanning electron micrograph of $(NH_4)Fe(PO_4) \cdot H_2O$ (×3000).
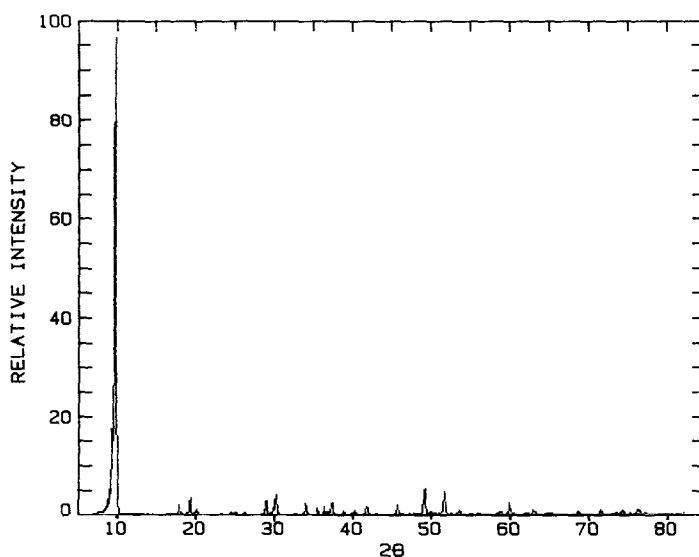
FIG. 2. X-ray powder pattern for $(NH_4)Fe(PO_4) \cdot H_2O$ crystallites on a flat glass slide, Cu$K\alpha$ radiation. The strong reflection is (010).

orientation to X-ray diffraction analysis as shown in Fig. 2. From these data, which show a strongly enhanced (010) reflection, it is clear that the crystallites are oriented with the b-axis predominately normal to the plane of the glass slide. X-ray patterns of the surfaces of pressed pellets showed similar orientation with respect to the pellet surface. This feature was exploited in performing the bulk magnetic and Mössbauer effect experiments.

Magnetic Properties

Magnetic data were collected on disk-shaped, pressed samples which exhibited considerable crystallographic texture, the b-axis being normal to the pellet surface. Figure 3 shows magnetic susceptibility data for two orientations of the applied field, parallel and perpendicular to the b-axis. Both curves show three distinct regions as a function of temperature, a Curie–Weiss region down to 80 K (I); a range between 70 and about 25 K where Curie–Weiss deviations, presumably due to short-range order,

are found (II); and a region of apparent long-range magnetic order below 25 K (III). Concerning region I, there is a small anisotropy, the susceptibility perpendicular to b being slightly higher than χ parallel to b. The Curie constants and effective magnetic moments are nearly the same, 3.55(5) cm^3 mole^{-1} K^{-1} and 5.33(5) μ_B for $\chi\|b$ and 3.67(5) cm^3 mole^{-1} K^{-1} and 5.41(5) μ_B for $\chi\perp b$. These values are consistent with high-spin Fe^{2+}. The Weiss constants, θ_c, are also similar $-69(1)$ K and $-64(1)$ K for $\chi\|b$ and $\chi\perp b$, respectively. Examination of region II indicates that the Curie–Weiss deviations are of opposite sign for the two susceptibilities, being negative (lower χ) for $\chi\|b$ and positive (higher χ) for $\chi\perp b$. Thus, the short-range order is antiferromagnetic parallel to b which is the interlayer direction and ferromagnetic perpendicular to b or within the layers.

The transitions between regions I, II, and III are shown more clearly in Fig. 4. Note especially the sharp increase in both susceptibility components beginning near 26 K
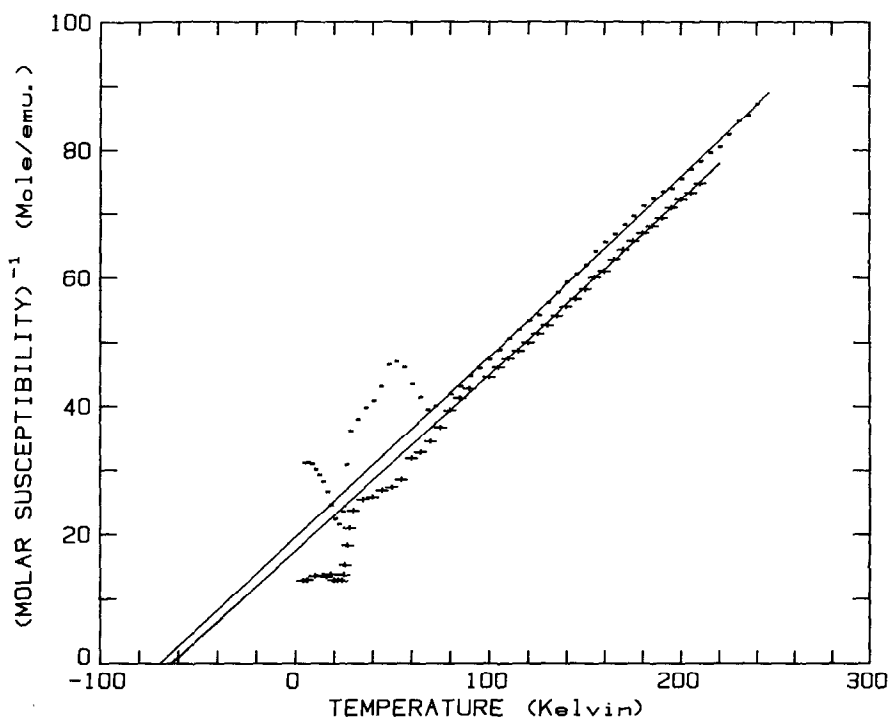
FIG. 3. Inverse magnetic susceptibility as a function of temperature for oriented polycrystalline samples of $(NH_4)Fe(PO_4) \cdot H_2O$. Applied field (1.0 T) parallel to b (●) and perpendicular to b (+). The lines are Curie–Weiss fits to the high-temperature data.

and peaking at 22 to 24 K. This suggests that the transition to the long-range ordered state is first order. The clear maximum in the $\chi\|b$ data is typical of an uniaxial antiferromagnet with the field parallel to the preferred axis and the nearly constant susceptibility below 23 K for $\chi\perp b$ is characteristic for the field normal to the easy direction. However, $\chi\|b$ does not fall to zero as would be expected for a simple uniaxial antiferromagnet. This may reflect significant crystallographic disorder in the pressed pellets relative to a perfect single crystal but further studies seem to indicate another explanation.

Evidence that this material is not a simple uniaxial antiferromagnet in the ordered state is available in Figs. 5 and 6. Figure 5 shows the existence of a weak spontaneous

magnetization for both orientations of the small, 5×10^{-3} T, applied field indicating some form of sublattice moment canting or misalignment. The spontaneous moment is about twice as great normal to b as parallel to b. The isothermal (4.2 K) demagnetization data of Fig. 6 indicate a remnant moment, again for both orientations of the field with respect to the b-axis. Note that the shape of the M vs H curves apart from the remnant moment is again typical for an uniaxial antiferromagnet. The "hard-axis" curve is linear reflecting the constant susceptibility and the easy axis curve is relatively flat at low fields but tends upward at higher fields indicating some misalignment or the onset of a spin-flop transition. All of this behavior is, however, superimposed on a remnant magnetic moment.
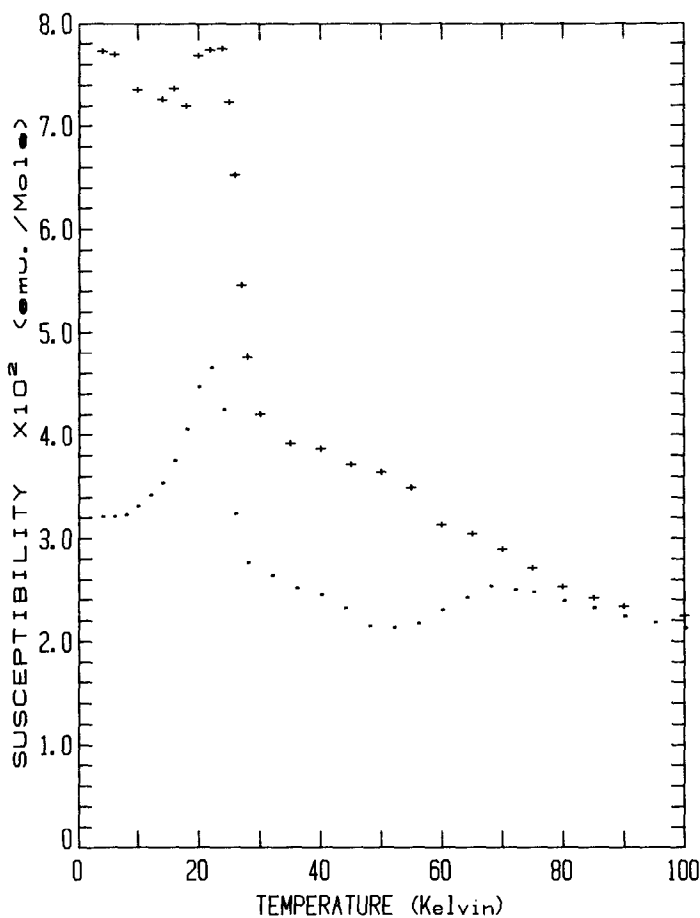
FIG. 4. Magnetic susceptibility of oriented (NH₄)Fe(PO₄) · H₂O in the low-temperature region. Applied field (1.0 T) parallel to *b* (●) and perpendicular to *b* (+).

To summarize the picture which emerges from qualitative analysis of the bulk magnetic data, (NH₄)Fe(PO₄) · H₂O is approximately a uniaxial antiferromagnet below 26 K with the direction nearly parallel to the *b*-crystallographic axis. The antiferromagnetic behavior is superimposed on a more or less constant spontaneous magnetization due, presumably, to sublattice canting or misalignment. The transition to the long-range ordered state is abrupt in temperature and possibly first order. From the short-range ordered region between 26 and 70 K one can infer ferromagnetic intralayer ex-

change and antiferromagnetic interlayer exchange interactions.

Mössbauer Effect

The spectrum of the oriented sample was recorded at room temperature with the plane of the sample perpendicular to the γ-ray direction and the unequal intensities of the resulting two lines of the quadrupole doublet bore out the oriented nature of the sample (Fig. 7a). Tilting the sample through an angle of 45° changed the relative intensities of these lines (Fig. 7b) and hence confirmed that the sample was indeed oriented.

Further support came from the spectrum of the random sample where the two doublet lines were of almost equal intensity (Fig. 8). Close examination of these spectra revealed the presence of a small amount of Fe^{3+} in the sample and this was allowed for in the fitting of the spectrum in Fig. 8 and all subsequent fits. The random sample was then placed in the cryostat and a series of spectra measured at temperatures from 6 to 150 K. At 6 K the spectrum was typical of a magnetically ordered Fe^{2+} in an electric field gradient. Because of the similar magnitudes of the magnetic and quadrupole interactions the normally forbidden $\Delta M = \pm 2$ transitions are visible (Fig. 9), indicating that V_{zz} and $\langle H \rangle$ are not coaxial. Raising the temperature results in the diminution of the magnetic field which collapses completely at ~26 K. All of the analyzed data are summarized in Table I and some representative spectra are shown in Figs. 7–9. It is clear that the dominant spectral component is due to high-spin Fe^{2+}. A small amount of a Fe^{3+} doublet is present, visible in Figs. 7 and 9c, which remains magnetically unsplit at least at 6 K, which we conclude is an impurity and not part of the structure of the
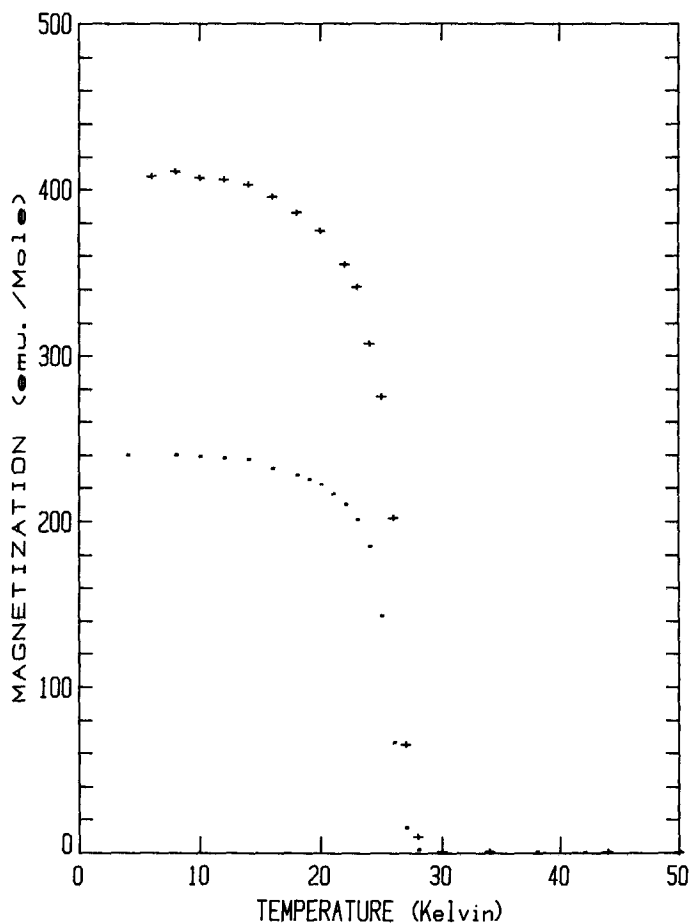

FIG. 5. Spontaneous magnetization versus temperature of an oriented sample of $(NH_4)Fe(PO_4) \cdot H_2O$ in an applied field of 0.005 T with the field parallel to b (●) and perpendicular to b (+).
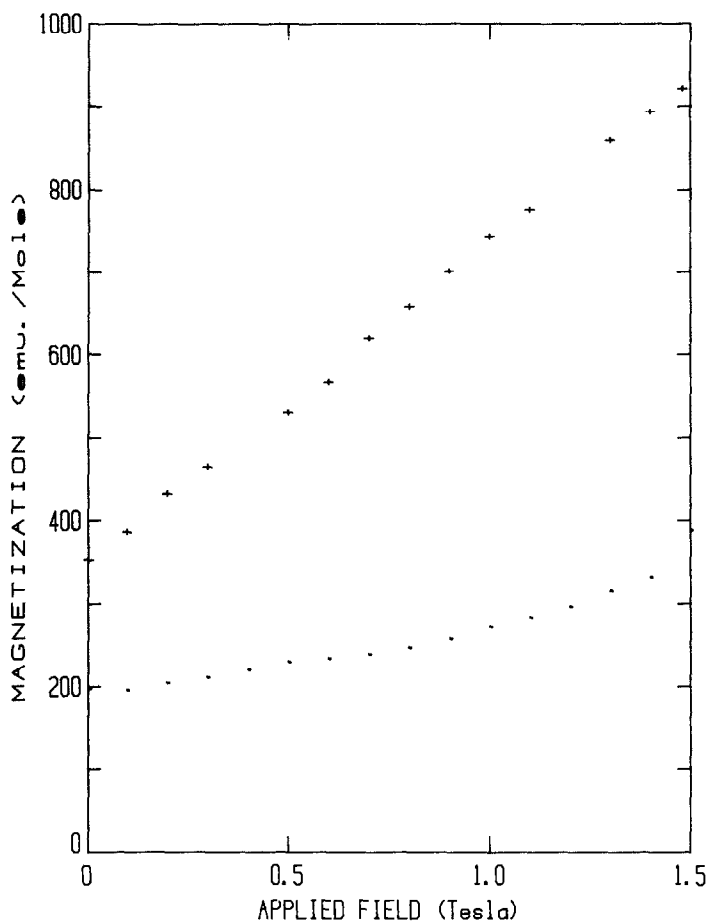
FIG. 6. Demagnetization curves at 4.2 K for oriented samples of $(NH_4)Fe(PO_4) \cdot H_2O$. Applied field parallel to b (●) and perpendicular to b (+).

compound under investigation. From the magnetically split spectra, which clearly exhibit the normally "forbidden" lines, we are able to determine the sign of the quadrupole coupling constant, the value of the asymmetry parameter η, and a value for the polar angle θ between the principal component of the EFG tensor and the effective hyperfine magnetic field. Unfortunately, the azimuthal angle ϕ cannot be determined due to the small value of the η parameter. Actually this value is small enough so that the quadrupole coupling constant or split-

ting, Δ, can be used interchangeably. Knowledge of the sign of the EFG tensor and the value for η allowed us to determine the angle between V_{zz} and the crystal b-axis, which is along the beam direction, from the oriented sample spectrum. This angle appears to be 50° (5). The transition between the magnetically ordered and disordered states is clearly of the first order (Fig. 10). However, we were unable to find evidence for any hysteresis due to the sharpness of the transition. The bars on the data points in Fig. 10 represent the distribu-
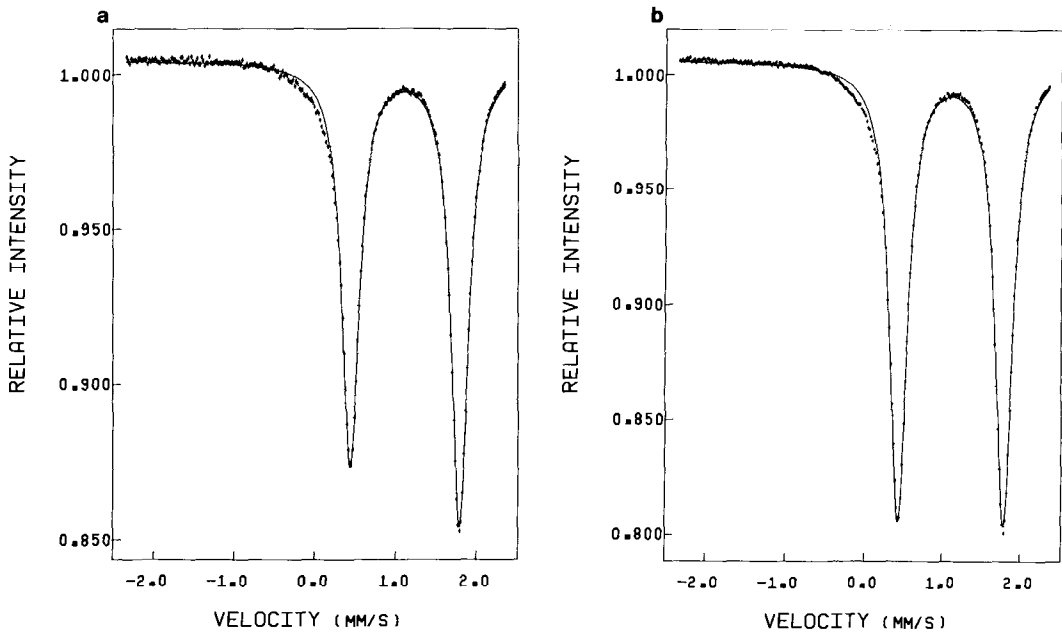
FIG. 7. (a) Room-temperature Mössbauer spectrum of an oriented sample of $(NH_4)Fe(PO_4) \cdot H_2O$ at 90°. Crystal b-axis is parallel to γ-ray direction. (b) Room-temperature Mössbauer spectrum of the same sample as (a) with the crystal b-axis 45° to the γ-ray direction.

tion of magnetic fields as estimated from the fitted second moment (4, 5). This field distribution we believe to be the result of a small temperature inhomogeneity across the sample rather than an intrinsic property of the sample.

The quadrupole coupling constant is strongly temperature dependent (Fig. 11) but no significant change in this parameter was observed at the magnetic ordering temperature. It is evident that the first excited crystal field level is about 50 K above the ground state level and that a few additional levels are probably available between this and room temperature. This finding implies that the Fe^{2+} moments in this compound are Heisenberg-like rather than Ising. This is consistent with the essentially isotropic susceptibility reported in the preceding section. It is important to note that no hyperfine magnetic interaction occurs, at least on the Mössbauer time scale, above the transi-
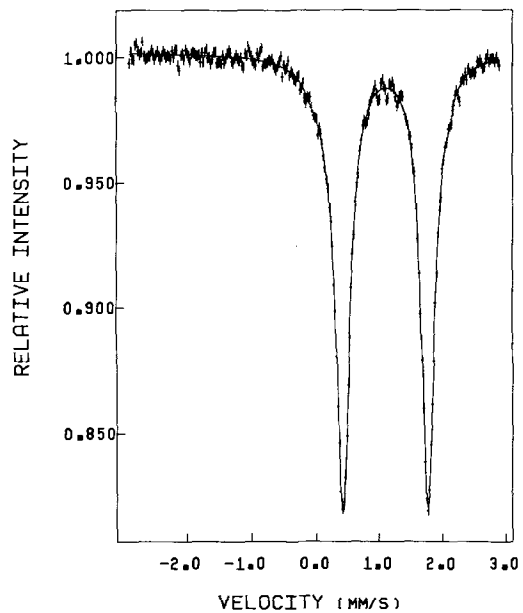

FIG. 8. Room-temperature Mössbauer spectrum of a "random" sample of $(NH_4)Fe(PO_4) \cdot H_2O$ at 90°. Absorber plane normal to the beam.
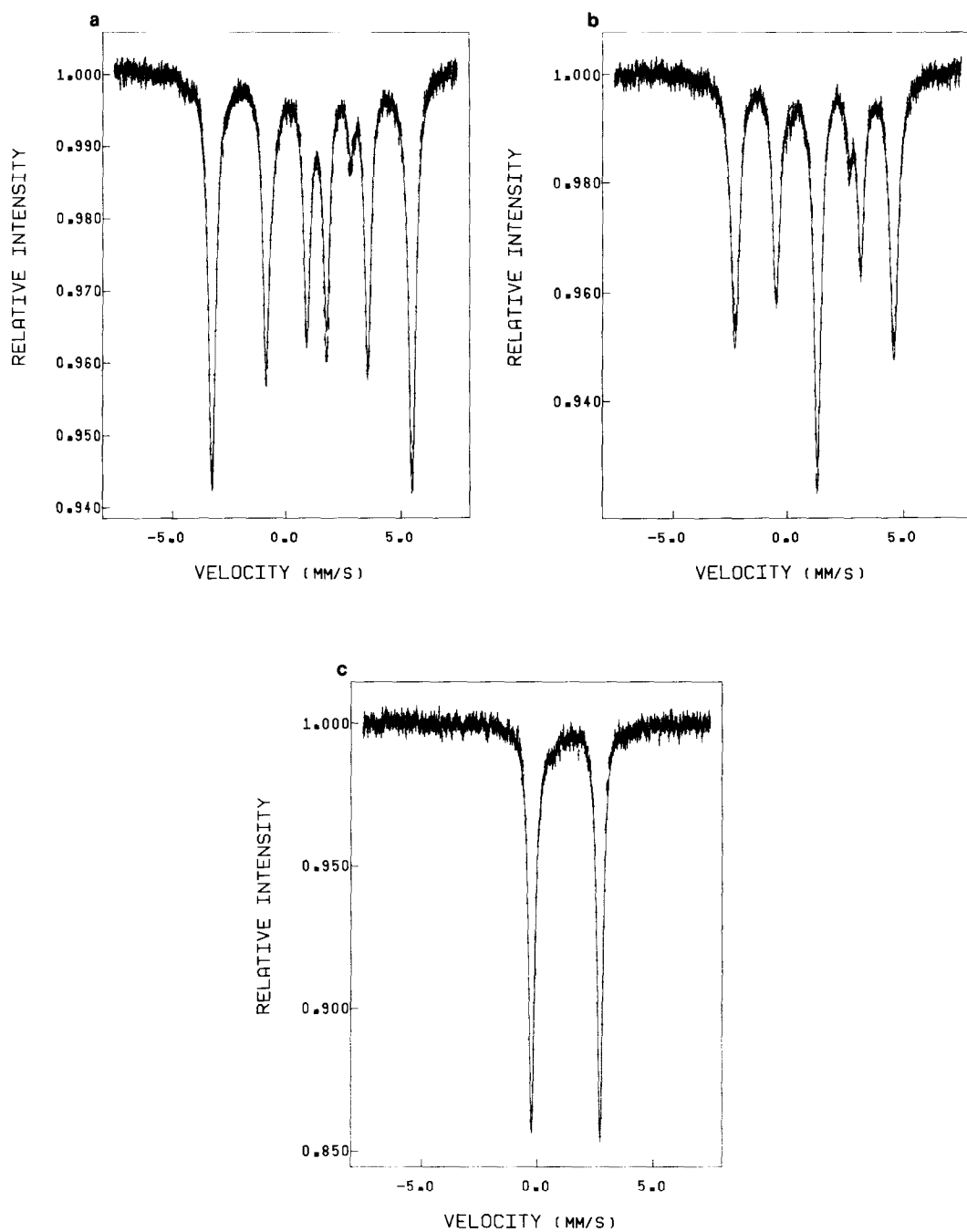
FIG. 9. Variable-temperature Mössbauer spectra of the random sample. (a) 6 K; (b) 23.3 K; (c) 27.9 K.

GREEDAN ET AL.

TABLE I

RELEVANT HYPERFINE PARAMETERS FOR $(NH_4)Fe(PO_4) \cdot H_2O$

T (K)	$\langle H \rangle$ (T)	$\frac{1}{2}eQV_{zz}$ (ch^{-1} w$_0^{-1}$) (mm/sec)	θ (deg)	η	δ^a (mm/sec)
6(1)	22.3(1)	2.96(1)	62(2)	0.06(1)	1.34(1)
14.8(1)	21.8(1)	2.95(1)	62(2)	0.06(1)	1.33(1)
21.9(1)	19.4(1)	2.94(1)	62(2)	0.07(1)	1.34(1)
22.3(1)	19.1(1)	2.94(1)	62(2)	0.07(1)	1.34(1)
22.8(1)	18.7(1)	2.95(1)	62(2)	0.06(1)	1.34(1)
23.3(1)	15.6(1)	2.98(3)	62(2)	0.06(const)	1.34(1)
24.8(1)	12.9	2.95(const)	62(const)	0.06(const)	1.32(2)
27.9(1)	0	2.94(1)	—	0.06(const)	1.34(1)
77(1)	0	2.81(1)	—	0.06(const)	1.31(1)
100(1)	0	2.77(1)	—	0.06(const)	1.30(1)
150(1)	0	2.57(1)	—	0.06(const)	1.22(1)
295(2)	0	1.34(1)	—	0.06(const)	1.22(1)

^{a} Isomer shift reported versus room-temperature α-Fe.

tion due to three-dimensional ordering at 26 K although short-range order effects were observed in the static susceptibility.

We have performed point charge calculations in order to estimate the directions of the principal EFG components. The room-temperature lattice constants reported in an earlier section were used while the fractional atomic positions were taken from the $(NH_4)Cd(PO_4) \cdot H_2O$ compound (3). The charges within and on the boundary of the oxygen octahedron were included in the calculation. It was necessary to move some charge from the closest oxygens toward the
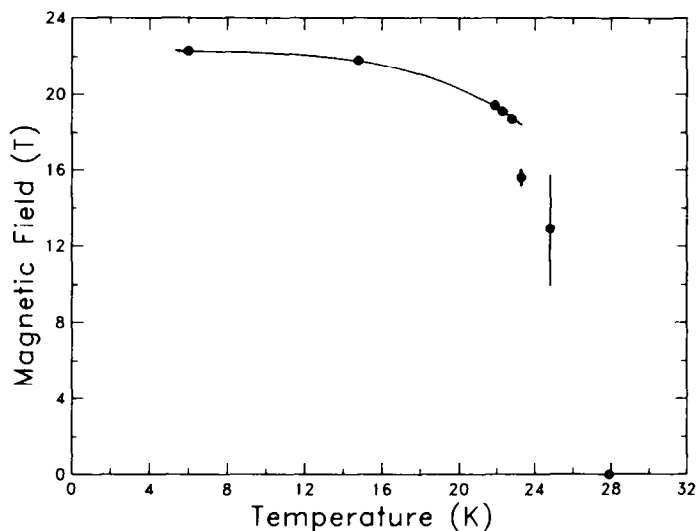

FIG. 10. Temperature dependence of the hyperfine field for $(NH_4)Fe(PO_4) \cdot H_2O$.
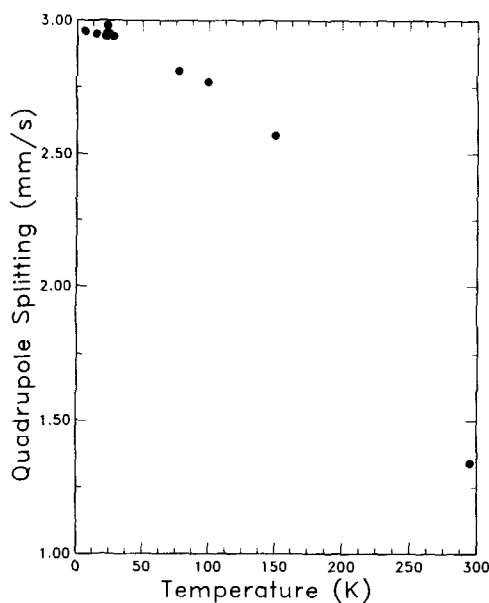
FIG. 11. Temperature dependence of the quadrupole splitting.

Fe^{2+} to allow for covalency effects. Such a model produced a positive coupling constant, an η value of 0.07, and a V_{zz} lying in the b–c plane at an angle 44° from the inverted b-axis in the direction of the c-axis. The value measured by Mössbauer spectroscopy is 50°. The magnetic data (Figs. 4 and 6) indicate that the easy axis of magnetization is not very far from the b-axis. The Mössbauer results give a value for smallest angle between the hyperfine field direction and the crystal b-axis of 12° (5) considering statistical errors only. Given that the sample itself is not a true single crystal and that sublattice canting clearly exists, the Mössbauer and bulk magnetic results are consistent. If any appreciable spin canting, greater than about 5°, is present it affects only the azimuthal angle ϕ as the magnetically split spectra can be described by the otherwise unique set of hyperfine parameters. The angle ϕ cannot be determined due to the almost axial symmetry of the EFG tensor as noted above.

Summary and Conclusions

(NH₄)Fe(PO₄) · H₂O appears to be structurally related to the compounds (NH₄)Co(PO₄) · H₂O and (NH₄)Cd(PO₄) · H₂O which have a structure in which corner-shared layers of MO_6 octahedra are separated by NH₄⁺ groups along a uniqe crystallographic axis. The magnetic properties of (NH₄)Fe(PO₄) · H₂O are complex. With respect to bulk magnetism there are three distinct temperature regimes, a paramagnetic Curie–Weiss region $T > 70$ K, a short-range ordered region 26 K $< T < 70$ K, and a long-range ordered region below 26 K. Measurements on highly oriented polycrystalline samples show essentially isotropic paramagnetic behavior. The temperature dependence of the quadrupolar interaction derived from Mössbauer data indicate the presence of a number of crystal field levels at energies between 50 and 300 K above the ground state. Both of these observations are consistent with a Heisenberg model for the Fe^{2+} moment in this compound. Deviations from the Curie–Weiss behavior in the short-range ordered region shows that the interlayer exchange is antiferromagnetic while the intralayer interaction is ferromagnetic. The rate of magnetic fluctuations in this regime is faster than the Mössbauer time scale as no magnetic hyperfine interaction is detected. The transition to the long-range ordered state at 26 K is clearly first order as seen from the temperature dependence of the Mössbauer hyperfine field. The ordered state is approximately an uniaxial antiferromagnet with the easy axis nearly parallel to the layer stacking direction, but with sublattice canting or misalignment which produces a weak spontaneous magnetization.

Among the issues which are not well-understood is the origin of the first-order magnetic transition and the reason for the frustrated behavior evidenced in the short-range ordered regime. One possible origin

of both features might be associated with the NH_4^+ ions which provide the superexchange links between layers. These pathways must involve hydrogen bonds with the O atoms of the phosphate groups. If the NH_4^+ groups are rotating or librating the interlayer exchange could be frustrated. When this motion ceases, an abrupt transition to a long-range antiferromagnetic state is possible. A detailed structure determination of this material at various temperatures would be necessary to test this hypothesis.

Acknowledgments

References

1. D. TRANQUI, A. DURIF, J.-C. GUITEL, AND M. T. AVERBUCH-POUCHOT, *Bull. Soc. Fr. Miner. Cristallogr.* **91**, 10 (1968).
2. A. DURIF AND M. T. AVERBUCH-POUCHOT, *Bull. Soc. Fr. Miner. Cristallogr.* **91**, 495 (1968).
3. YU. A. IVANOV, M. A. SIMONOV, AND N. V. BELOV, *Sov. Phys. Crystallogr.* **21**, 109 (1976).
4. K. REUBENBAUER AND T. BIRCHALL, *Hyperfine Interact.* **7**, 125 (1979).
5. G. CZJZEK AND W. BERGER, *Phys. Rev. B.* **1**, 957 (1970).